Journal of Industrial Microbiology & Biotechnology (2019) 46:1631–1641
https://doi.org/10.1007/s10295-019-02237-8

SIMB
Society for Industrial Microbiology and Biotechnology

BIOCATALYSIS - ORIGINAL PAPER

Integrating enzyme evolution and high-throughput screening for efficient biosynthesis of L-DOPA

Weizhu Zeng[1,2] · Bingbing Xu[1,2,4] · Guocheng Du[1,3] · Jian Chen[1,2,4] · Jingwen Zhou[1,2,4]

Received: 12 June 2019 / Accepted: 11 September 2019 / Published online: 18 September 2019

Abstract

L-DOPA is a key pharmaceutical agent for treating Parkinson's, and market demand has exploded due to the aging population. There are several challenges associated with the chemical synthesis of L-DOPA, including complicated operation, harsh conditions, and serious pollution. A biocatalysis route for L-DOPA production is promising, especially via a route catalyzed by tyrosine phenol lyase (TPL). In this study, using TPL derived from *Erwinia herbicola* (*Eh*-TPL), a mutant *Eh*-TPL was obtained by integrating enzyme evolution and high-throughput screening methods. L-DOPA production using recombinant *Escherichia coli* BL21 (DE3) cells harbouring mutant *Eh*-TPL was enhanced by 36.5% in shake flasks, and the temperature range and alkali resistance of the *Eh*-TPL mutant were promoted. Sequence analysis revealed two mutated amino acids in the mutant (S20C and N161S), which reduced the length of a hydrogen bond and generated new hydrogen bonds. Using a fed-batch mode for whole-cell catalysis in a 5 L bioreactor, the titre of L-DOPA reached 69.1 g L^{-1} with high productivity of 11.52 g L^{-1} h^{-1}, demonstrating the great potential of *Eh*-TPL variants for industrial production of L-DOPA.

Keywords Error-prone PCR · High-throughput screening · Tyrosine phenol lyase · Catalytic activity · Fed-batch mode

Introduction

L-DOPA is a major pharmaceutical agent for treatment of Parkinson's disease, a neurodegenerative disorder commonly occurring in the elderly. The demand for L-DOPA is increasing with an aging population [6, 26]. L-DOPA can be produced by plant extraction, chemical synthesis, and biotechnological routes [50, 51]. Plant extraction commonly uses cat beans, faba bean, or quinoa as raw materials, from which L-DOPA is extracted by membrane separation techniques [15, 35]. This route is difficult to industrialise at a large scale due to limitations of materials, high cost, and low productivity [30]. Chemical synthesis involves eight reaction steps and usually uses vanilla phenol and acetyl urea as substrates [49]. L-DOPA produced by chemical methods is characterised by high purity, high yield, and minimal intermediate by-products, but several drawbacks exist, including complicated production processes, harsh reaction conditions, and serious environmental pollution [38, 49]. Consequently, biotechnological routes are considered an ecologically and attractive choice, especially biological fermentation and whole-cell catalysis methods [10, 20].

Whole-cell catalysis methods for L-DOPA production have attracted much attention. Previous research showed that various enzymes can be used for this process, including tyrosinase, aminoacylase, and tyrosine phenol lyase [13, 30]. The enzyme tyrosinase isolated from *Acremonium rutilum* can catalyze the conversion of L-tyrosine to L-DOPA [23]. However, this enzyme also possesses both monophenol oxidase activity and bisphenol oxidase activities. L-tyrosine

Electronic supplementary material The online version of this article (https://doi.org/10.1007/s10295-019-02237-8) contains supplementary material, which is available to authorized users.

✉ Jingwen Zhou
zhoujw1982@jiangnan.edu.cn

1 Key Laboratory of Industrial Biotechnology, Ministry of Education and School of Biotechnology, Jiangnan University, 1800 Lihu Road, Wuxi 214122, Jiangsu, China

2 National Engineering Laboratory for Cereal Fermentation Technology, Jiangnan University, 1800 Lihu Road, Wuxi 214122, Jiangsu, China

3 The Key Laboratory of Carbohydrate Chemistry and Biotechnology, Ministry of Education, School of Biotechnology, Jiangnan University, Wuxi 214122, China

4 Jiangsu Provisional Research Center for Bioactive Product Processing Technology, Jiangnan University, 1800 Lihu Road, Wuxi 214122, Jiangsu, China

can be oxidized to L-DOPA and further to dopaquinone and dopachrome, which requires the addition of large quantities of reducing agents to stop this transformation reaction [36]. More importantly, it is difficult to separate residual L-tyrosine and the L-DOPA product due to the high similarity between these two substrates in terms of structure and properties. Aminoacylase can catalyze the conversion of L-glutamate or L-aspartate to L-DOPA, as reported for a transaminase from *Alcaligenes faecalis* [48]. However, further research on this route has not been forthcoming. Tyrosine phenol lyase (TPL) has been applied for L-DOPA production using a whole-cell catalysis method [21, 29].

TPL naturally catalyzes the β-elimination of L-tyrosine to pyruvate, phenol, and ammonium using the cofactor pyridoxal 5′-phosphate (PLP), and the reaction is reversible [21, 34]. TPL has been widely utilised for the synthesis of aromatic amino acids and their derivatives such as L-DOPA that can be synthesised from pyruvate, catechol, and ammonia as substrates [39]. TPL enzymes with high catalytic activity have been reported from several microbes including *Citrobacter freundii* [7], *E. herbicola* [22], and *Fusobacterium nucleatum* [46]. The performance of these different TPLs recombinantly expressed in *Escherichia coli* has been compared for the synthesis of L-DOPA in whole-cell catalysis, and attempts have been made to enhance catalytic activity via random mutations and transcriptional regulation [19, 23].

In the present study, enzyme evolution and high-throughput screening methods were integrated to screen mutant TPLs with good performance for the synthesis of L-DOPA, using native TPL derived from *E. herbicola*. A mutant *Eh*-TPL was generated after two rounds of error-prone PCR (epPCR), and whole-cell catalysis with recombinant *E. coli* BL21 (DE3) harbouring mutant *Eh*-TPL resulted in accumulation of L-DOPA reaching 18.2 g L^{-1} in shake flasks, an increase by 36.5% compared with wild-type (WT) TPL. The temperature range and alkali resistance of mutant *Eh*-TPL were enhanced. Two amino acids (S20C and N161S) are mutated in the enzyme variant, which reduced the length of hydrogen bond and formed new hydrogen bonds. A fed-batch mode whole-cell catalysis procedure for L-DOPA synthesis was established in a 5 L bioreactor, and the titre of L-DOPA reached 69.1 g L^{-1} with productivity up to 11.52 g L^{-1} h^{-1}. Thus, *Eh*-TPL mutant could prove to be useful biocatalysts for industrial production of L-DOPA.

Materials and methods

Strains and plasmids

Escherichia coli BL21 (DE3) and plasmid pET-28a(+) were used as the host and expression vector, respectively. The pET-28a(+)-*Eh*-TPL construct expressing TPL from *E. herbicola* was prepared in the previous work [53].

Media and culture conditions

The medium for seed and slant cultures [Luria–Bertani (LB) medium] contained 10 g L^{-1} peptone, 5 g L^{-1} yeast extract, 10 g L^{-1} NaCl, and 50 μg mL^{-1} kanamycin. In addition, 20 g L^{-1} agar was added to slant medium. The complete fermentation medium contained 5 g L^{-1} glycerol, 12 g L^{-1} peptone, 24 g L^{-1} yeast extract, 2.31 g L^{-1} KH_2PO_4, 16.37 g L^{-1} K_2HPO_4, 1.1 g L^{-1} citric acid monohydrate, 1 g L^{-1} $MgSO_4{\cdot}7H_2O$, and 1 mL trace-element solution. Trace-element solution was dissolved in 1 mol L^{-1} HCl containing 0.2 g L^{-1} $CuCl_2{\cdot}2H_2O$, 0.3 g L^{-1} $ZnSO_4{\cdot}7H_2O$, 1.5 g L^{-1} $CaCl_2{\cdot}2H_2O$, 2.8 g L^{-1} $CoSO_4{\cdot}7H_2O$, 2.8 g L^{-1} $FeSO_4{\cdot}7H_2O$, and 2.0 g L^{-1} $MnCl{\cdot}4H_2O$.

The strain preserved in glycerol was inoculated onto a solid LB medium plate and incubated at 37 °C for 24 h. The seed culture was grown in 250 mL flasks containing 25 mL culture medium at 37 °C on a reciprocal shaker at 220 rpm. Flask cultures were grown in 500 mL flasks containing 50 mL culture medium at 37 °C with a 1% (v/v) inoculum. When the absorbance of the cell culture at 600 nm (OD_{600}) reached 0.6–0.8, the culture temperature was adjusted to 25 °C, 0.2 mmol L^{-1} isopropyL-β-D-thiogalactoside (IPTG) was added, and culturing was continued for 8 h. Fed-batch fermentation was performed in a 5 L fermenter (T&J Bioengineering, Shanghai, China) containing a 2.5 L initial working volume with shaking at 400 rpm and 1 vvm with a 2% inoculum. When the OD_{600} reached 12–14, the culture temperature was adjusted to 25 °C, 0.2 mmol L^{-1} IPTG was added, and fermentation was continued for 8 h. The pH was maintained at 7.0 with 25% ammonia solution and 25% phosphoric acid solution. All fermentation processes were performed in triplicate and the results are presented as mean values.

Preparation of biocatalyst and synthesis of L-DOPA

The whole-cell catalyst was harvested after centrifuging the fermentation broth at 5000 rpm for 10 min at 4 °C and washing twice with 0.2 mol L^{-1} phosphate buffer. The reaction mixture for the synthesis of L-DOPA was composed of 18 g L^{-1} sodium pyruvate, 10 g L^{-1} catechol, 30 g L^{-1} ammonium acetate, 2 g L^{-1} EDTA, and 4 g L^{-1} Na_2SO_3. The pH was adjusted to 9.0 with 25% ammonia solution. Biomass was added to 6 g L^{-1} (wet weight) and the reaction was conducted at 20 °C with shaking at 180 rpm in shake flasks or a 5 L bioreactor.

Mutant library construction by epPCR

Random mutagenesis of TPL was carried out by epPCR with recombinant plasmid pET-28a (+)-*Eh-TPL* as template. Upstream and downstream primers for *Eh-TPL* were *TP*L-F (5′-CGCGGATCCATGAACTATCCGGCAGAACCGT-3′) and *TP*L-R (5′-CCCAAGCTTTTAGATGAAGTCGAA ACGCGCG-3′). The reaction system for epPCR is shown in Table 1. A total of 30 cycles were performed with pre-denaturation at 94 °C for 5 min, denaturation at 94 °C for 30 s, primer annealing at 64 °C for 30 s, and elongation at 72 °C for 2 min. After amplification, PCR products were digested with *Bam*HI and *Hind*III, purified, and ligated into the pET28a(+) expression vector previously digested with *Bam*HI and *Hind*III. The mutant library was constructed by ligating products and transforming into *E. coli* BL21 (DE3) by electroporation. Purification of PCR products was carried out using an UNIQ-10 Column MicroDNA Gel Extraction Kit (Sangon Biotech, Shanghai, China). The mutation rate was the average value calculated by randomly selecting 8 mutants from each group of mutation libraries after gene sequencing.

High-throughput screening of mutants

The engineered strains containing mutant *Eh-TPL* enzymes plated on solid LB media were cultivated at 37 °C for 24 h. Colonies were picked and transferred to 96-shallow-well microtiter plates (MTPs) containing 200 μL LB liquid medium for further screening by the QPix 420 system (Molecular Devices, Sunnyvale, CA). A 20 μL sample of seed liquid cultivated at 37 °C for 8–10 h was transferred from 96-shallow-well MTPs to 96-deep-well MTPs containing 600 μL of fermentation medium. After cultivating for 2 h, the temperature was adjusted to 25 °C and IPTG was added to induce TPL expression for 10 h at 900 rpm on a Titramax 1000 multi-plate shaker (Heidolph, Schwabach, Germany).

All 96-deep-well MTPs were centrifuged in a 96-well MTP centrifuge (Beckman, Brea, CA) at 5000 rpm for 10 min, and supernatants were removed. A 400 μL sample of reaction mixture was immediately added to each well using a 96-channel pipette (RockGeneBio, Shanghai, China) and reacted for 4 h at 15 °C and 220 rpm. Aliquots (10 μL) of supernatants were transferred to normal 96-well MTPs after centrifuging, 90 μL of salicylaldehyde (5%, v/v) and 100 μL of NaOH solution (75 g L^{-1}) were added to each well, and the absorbance was measured at 465 nm using a Multiskan FC microplate reader (Thermo Fisher, Waltham, MA). Mutants with high TPL activity were identified based on absorbance, since higher TPL activity corresponded to lower absorbance. The best mutant was confirmed by secondary screening in shake flasks and used for expression and purification of mutant TPL.

Table 1 Mutation rate of epPCR with different concentrations of Mg^{2+} and Mn^{2+}

Combinations of Mg^{2+} and Mn^{2+}	Mutation rate (%)
2.0 mmol L^{-1} Mg^{2+} and 0.1 mmol L^{-1} Mn^{2+}	0.13
2.0 mmol L^{-1} Mg^{2+} and 0.2 mmol L^{-1} Mn^{2+}	0.18
2.0 mmol L^{-1} Mg^{2+} and 0.3 mmol L^{-1} Mn^{2+}	0.24
2.0 mmol L^{-1} Mg^{2+} and 0.4 mmol L^{-1} Mn^{2+}	0.37
2.0 mmol L^{-1} Mg^{2+} and 0.5 mmol L^{-1} Mn^{2+}	0.41
4.0 mmol L^{-1} Mg^{2+} and 0.1 mmol L^{-1} Mn^{2+}	0.26
4.0 mmol L^{-1} Mg^{2+} and 0.2 mmol L^{-1} Mn^{2+}	0.52
4.0 mmol L^{-1} Mg^{2+} and 0.3 mmol L^{-1} Mn^{2+}	0.78
4.0 mmol L^{-1} Mg^{2+} and 0.4 mmol L^{-1} Mn^{2+}	0.93
4.0 mmol L^{-1} Mg^{2+} and 0.5 mmol L^{-1} Mn^{2+}	1.05

TPL purification and analysis

Purification of TPL

Biomass was obtained by centrifuging the fermentation liquid at 5000 rpm for 10 min at 4 °C and washing twice with 0.2 mol L^{-1} phosphate buffer. Biomass was diluted to OD_{600} = 10 in 50 mmol L^{-1} potassium phosphate buffer (pH 8.0). Crude enzyme liquid was harvested by centrifuging for 10 min after ultrasonic fragmentation for 10 min (2 s pulses, 4 s pauses). TPL was purified from crude enzyme liquid using an AKTA purifier (GE Healthcare, Michigan, US) with a HiTrap nickel affinity column after filtering crude enzyme solution through a 0.22 μm inorganic membrane. Purification involved equilibrating the column with buffer A (3–5 column volumes), injecting 10 mL of sample, applying buffer A again (3–5 column volumes), and eluting with a linear gradient of buffer B. TPL was detected in eluted fractions by measuring UV absorbance of peaks and verified by sodium dodecyl sulphate polyacrylamide gel electrophoresis (SDS-PAGE).

Determination of TPL concentration and activity

The TPL concentration was determined using a BCA Protein Assay Kit (Beyotime, Shanghai, China) following the manufacturer's instructions. TPL, also known as β-tyrosinase, could catalyze L-tyrosine to phenol, ammonia, and pyruvate and the reaction is reversible. It was also reported that the enzyme could catalyze the L-DOPA formation and decomposition as the similarity between phenol and catechol. The assay method of TPL activity was mainly detected by positive response that decomposed the L-tyrosine/L-DOPA. In addition, L-DOPA could be easily oxidized and could cause large errors in enzyme activity determination. Therefore, TPL activity was

generally assayed by determination of pyruvate formed from L-tyrosine as substrate.

Determination of the enzymatic properties of TPL

The influence of temperature on TPL activity was investigated using the above reaction mixture at different temperatures (10–50 °C) and the maximum activity was defined as 100%. Residual activities were assayed to examine the thermo-stability of TPL after incubating at 10–60 °C for 12 h.

The influence of pH on TPL activity was investigated by dissolving substrates in buffers at different pH values (5.0–10.0), and maximum enzyme activity at 30 °C for 30 min was again defined as 100%. Residual activities were assayed to examine the pH stability of TPL after incubating at 5.0–10.0 for 60 min and immediately diluting with a 20-fold volume of potassium phosphate buffer (pH 8.5). All experiments were conducted in triplicate.

Kinetic analysis

TPL activity was determined after adding pure enzyme and different concentrations of sodium pyruvate (1–10 mmol L^{-1}). Double reciprocal plots were drawn according to the Lineweaver–Burk method and kinetic parameters (K_m, V_{max}, $k_{cat,}$ and k_{cat}/K_m) were calculated.

Determination of biomass concentration

The optical density of the culture broth was measured using a Biospec-1601 spectrophotometer (Shimadzu Co., Kyoto, Japan) at 600 nm after an appropriate dilution.

Determining the concentration of L-DOPA and catechol

Reactions were terminated by adding 1 mmol L^{-1} HCl, centrifuged, and diluted 20-fold to measure L-DOPA and catechol content by high-performance liquid chromatography (HPLC) using an Agilent C_{18} column (250 mm×4.6 mm, 5 µm internal diameter; Agilent, Palo Alto, CA, USA). The mobile phase was 2.4/97.6 acetonitrile/water (containing 0.08% v/v formic acid), the temperature of the column was maintained at 35 °C, and the flow rate was 1 mL min^{-1}. L-DOPA and catechol were detected using an Agilent 1260 UV absorbance detector at 280 nm (Agilent).

Results and discussion

Optimisation of epPCR for *Eh*-TPL mutant library construction

Directed evolution is a powerful strategy for protein modification based on mutation and recombination by epPCR and DNA shuffling [12, 32]. The method of epPCR employed in this study has been applied previously to enhance the performance of enzymes, including enzyme activity, and pH and temperature stability [3, 5]. Briefly, epPCR introduces random mutations into the target gene during amplification in abnormal reaction conditions, resulting in a mutant library. Commonly employed methods for epPCR include increasing the concentration of Mg^{2+}, adding Mn^{2+}, applying low fidelity enzymes, and changing the ratio of the four dNTPs in the system [8]. The key challenge in epPCR is achieving an appropriate mutation rate, and we adjusted the concentrations of Mg^{2+} and Mn^{2+} to achieve this in the present work.

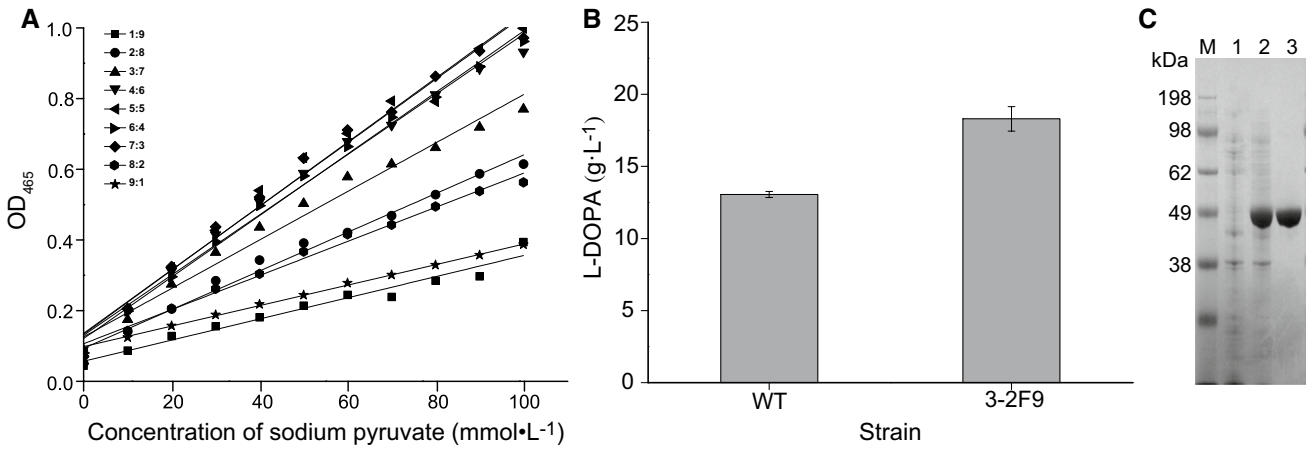

Fig. 1 Comparison of mutant and wild-type (WT) *Eh*-TPL enzymes. **a** Comparison of different ratios of salicylaldehyde and sodium pyruvate. A strong linear relationship was evident, represented by the equation $Y=0.00482X+0.10636$ ($R^2=0.99968$) when the volumetric ratio of salicycloaldehyde to sodium pyruvate was 9:1. Squares = 1:9; circles = 2:8; upward-pointing triangles = 3:7, downward-pointing triangles = 4:6, left-pointing triangles = 5:5, right-pointing triangles = 6:4, diamonds = 7:3, hexagons = 8:2, stars = 9:1. **b** Comparison of the titres of mutant and WT strains in shake flasks. Accumulation of L-DOPA was enhanced by 36.5%. **c** SDS-PAGE analysis of the purified *Eh*-TPL mutant. Lane M, protein markers; lane 1, *E. coli* BL21 (DE3)-pET28a(+); lane 2, crude enzyme from *E. coli* BL21(DE3)-pET28a(+)-*Eh*-TPL; lane 3, purified mutant *Eh*-TPL

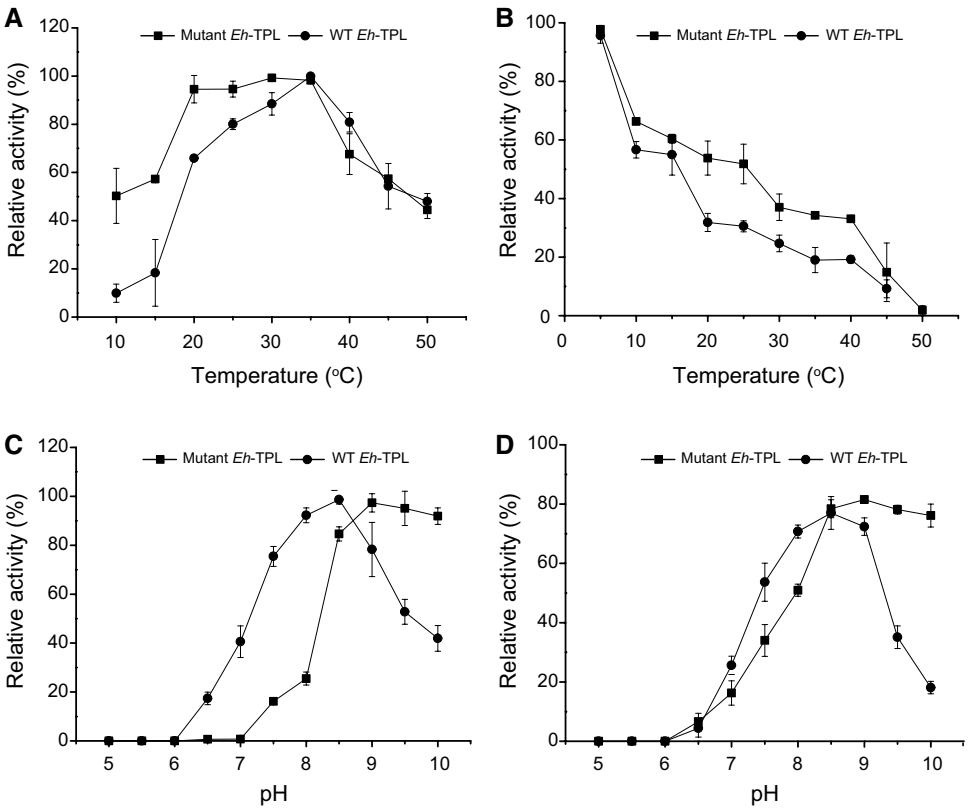

Fig. 2 Effects of temperature and pH on the catalytic activity of mutant *Eh*-TPL. High catalytic activity of mutant *Eh*-TPL can be maintained from 20 to 35 °C. The optimal pH for mutant *Eh*-TPL is pH 9.0, and 80% catalytic activity is maintained when the pH is > 9.0. The pH and temperature stability of mutant *Eh*-TPL is improved compared with that of WT *Eh*-TPL. **a** Analysis of optimal reaction temperature. **b** Temperature stability of WT and mutant *Eh*-TPL enzymes. **c** Analysis of optimal pH. **d** pH stability of WT and mutant *Eh*-TPL enzymes. Squares = mutant *Eh*-TPL; circles = WT *Eh*-TPL

The effects of different concentrations of Mg^{2+} (2.0–8.0 mmol L^{-1}) were explored and the results are shown in Figure S1A in Supplementary Material. Electrophoresis bands gradually darkened with increasing Mg^{2+} concentration, indicating that the efficiency of PCR was reduced with the increasing of Mg^{2+} concentration. To obtain relatively suitable efficiency of PCR, 2.0 or 4.0 mmol L^{-1} of Mg^{2+} were chosen for follow epPCR experiments. For more efficient selection of mutated *Eh*-TPL variants, the concentration of Mn^{2+} (0.1–1.0 mmol L^{-1}) was tested using the two optimal concentrations of Mg^{2+}. The results showed that electrophoresis band was brighter at 0.1–0.5 mmol L^{-1} Mg^{2+}, and darkened when the value exceeded 0.5 mmol L^{-1} (Fig. S1B in Supplementary Material). The mutant library was constructed by combining optimum Mg^{2+} (2 mmol L^{-1} and 4 mmol L^{-1}) and Mn^{2+} (0.1, 0.2, 0.3, 0.4, and 0.5 mmol L^{-1}) concentrations, and the mutation rate was calculated (Table 1). A principle mutation rate of no more than two or three amino acid changes per protein was suitable based on the length of the *Eh-TPL* gene (1377 bp). Treatment of concentrations of 4.0 mmol L^{-1} Mg^{2+} and 0.2 mmol L^{-1} Mn^{2+} was chosen resulting in a 0.52% mutation rate. A library of *Eh*-TPL mutants was constructed following various steps including restriction enzyme treatment, purification of digested DNA fragments, ligation, and transformation of the resulting constructs.

High-throughput screening of *Eh*-TPL-positive mutants

High-throughput screening is an effective strategy for identifying strains producing target products [40]. Equipment has been developed for this purpose, including the QPix microbial screening system, fluorescence-activated cell sorting systems, and microdroplet chips [27, 37]. This approach has been applied widely in basic and applied research, and combining it with various mutagenesis

Table 2 Kinetic parameters of WT and mutant *Eh*-TPL enzymes

Strain/parameter	K_m (mmol L^{-1})	V_{max} (μmol mg^{-1} min^{-1})	k_{cat} (s^{-1})	k_{cat}/K_m (s^{-1} mmol L^{-1})
Wild *Eh*-TPL	2.8 ± 0.2	35.7 ± 0.5	1.9 ± 0.2	0.68 ± 0.03
Mutant *Eh*-TPL	1.7 ± 0.3	42.6 ± 0.3	2.3 ± 0.1	1.35 ± 0.05

approaches can generate excellent strains with enhanced performance for production of target products, tolerance of harsh environmental conditions, and accumulation of non-native products or consumption of non-native substrates [9, 28]. Acetone can react with salicylaldehyde to produce a colour-developing chemical under strong alkaline conditions [47], and this has been used to establish a high-throughput screening method for TPL activity by optimising the addition of salicylaldehyde, the concentration of sodium pyruvate, and the reaction duration [46].

Herein, the volumetric ratio of sodium pyruvate (0–100 mmol L^{-1}) to salicylaldehyde (0.5%, v/v) was optimised to improve the sensitivity and accuracy of the screening procedure and the total volume of the mixture was 200 µL in 96-shallow well. The results revealed a strong linear relationship between OD_{465} and the concentration of sodium pyruvate, represented by the equation $Y = 0.00482X + 0.10636$ ($R^2 = 0.99968$) when the volumetric ratio of salicycloaldehyde to sodium pyruvate was 9:1 (Fig. 1a). Using this high-throughput screening method, positive mutant strain 3-2F9 was selected from a library containing 3×10^4 mutants resulting from two rounds of epPCR. After the secondary screening cultivated in shake flasks, the titre of L-DOPA produced by strain 3-2F9 was increased by 36.5% compared with the original strain (Fig. 1b). A bright electrophoresis band was present at ~ 49 kDa, consistent with

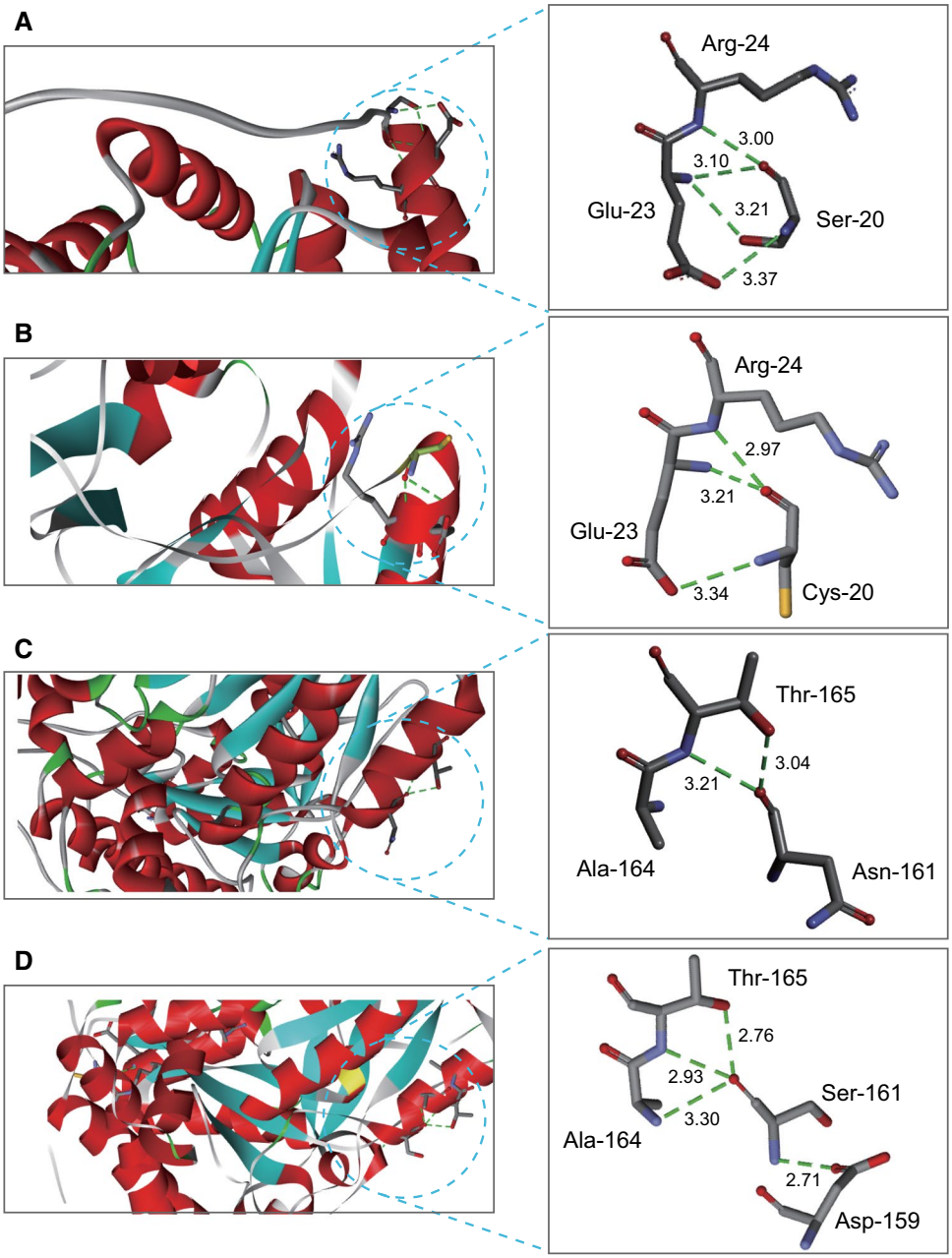

Fig. 3 Predicted structures of WT and mutant *Eh*-TPL enzymes. The number of hydrogen bonds in the vicinity of the Cys-20 residue in mutant *Eh*-TPL is decreased, and the length of hydrogen bonds between Glu-23 and ARG-24 is reduced. In addition, Cys-20 is a sulfur-containing amino acid in the N-terminal arm, and its presence results in two new hydrogen bonds formed between Asp-159 and Ala-164 with Ser-161 in mutant *Eh*-TPL. **a** Three-dimensional structure of WT *Eh*-TPL showing the region surrounding Ser-20. **b** Three-dimensional structure of mutant *Eh*-TPL showing the region surrounding Cys-20. **c** Three-dimensional structure of WT *Eh*-TPL showing the region surrounding Asn-161. **d** Three-dimensional structure of WT *Eh*-TPL showing the region surrounding Ser-161

the molecular weight of the TPL protein (52 kDa), indicating that the mutated TPL was successfully expressed (Fig. 1c).

Characterisation of *Eh*-TPL at different pH values and temperatures

The optimal reaction temperature and thermostability of WT and mutant *Eh*-TPL enzymes were investigated between 10 and 50 °C. The results showed that the optimal reaction temperature of the *Eh*-TPL mutant expressed by the strain 3-2F9 was 30 °C, compared with 35 °C for WT *Eh*-TPL expressed by the parent strain (Fig. 2a). The high catalytic activity of mutant *Eh*-TPL was maintained from 20 to 35 °C, but decreased significantly when the temperature was above 35 °C, whereas the activity of WT *Eh*-TPL was significantly reduced when the temperature was below or above 35 °C. The two enzymes were incubated at 10–50 °C for 12 h, and the remaining enzyme activity of the mutant was higher than that of WT *Eh*-TPL (Fig. 2b). The optimum temperature of TPL from *F. nucleatum* was previously determined to be 60 °C, and the catechol substrate and L-DOPA product were unstable under high temperature conditions [14]. In the present work, the *Eh*-TPL mutant retained high catalytic activity over a temperature range of 20–35 °C, which could be of benefit for L-DOPA production.

The effects of pH (5.0–10.0) on the activity of mutant and WT *Eh*-TPL were investigated, and the optimal pH of the mutant was 9.0, with 80% catalytic activity retained when the pH was above 9.0. In contrast, the optimal pH of WT *Eh*-TPL was 8.5, and enzyme activity decreased significantly when the pH was above 8.5 (Fig. 2c). The two enzymes were incubated at pH 5.0–10.0 for 60 min, and the remaining enzyme activity of the mutant was higher than that of the WT enzyme (Fig. 2d). During L-DOPA synthesis, the by-product tetrahydroisoquinoline can be formed from L-DOPA and sodium pyruvate through the Pictet–Spengler reaction [14, 45]. Accumulation of by-product could be affected by both temperature and pH, and high temperature can be a key factor. Determination of by-products of L-DOPA conversion liquid sample with LCMS–IT–TOF analysis is presented in Fig. S2 in Supplementary Material. Thus, considering the characteristics of enzyme responding to different pH and temperature, pH 9.0 and 20 °C were chosen for whole-cell catalysis of L-DOPA using mutant *Eh*-TPL in the present work.

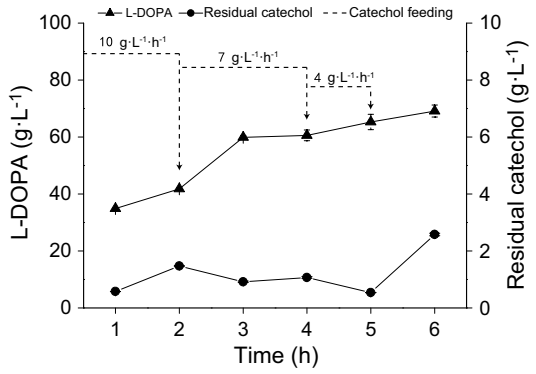

Fig. 4 Time course of L-DOPA biosynthesis using the established fed-batch mode. Whole-cell catalysis with strain 3-2F9 expressing mutant *Eh*-TPL was conducted in a 5 L bioreactor at 20 °C and 180 rpm. The initial concentrations of sodium pyruvate and catechol were 18 g L^{-1} and 10 g L^{-1}, respectively. Sodium pyruvate was added to 10 g L^{-1} h^{-1}, and catechol was added to 12 g L^{-1} h^{-1} from 0 to 2 h, 7 g L^{-1} h^{-1} from 2 to 4 h, and 4 g L^{-1} h^{-1} from 4 to 5 h. After reacting for 6 h, 69.1 g L^{-1} of L-DOPA was obtained, representing a productively of 11.52 g L^{-1} h^{-1}. Upward-pointing triangles = L-DOPA; circles = residual catechol

Characterisation of kinetic parameters and analysis of mutation sites

The TPL activity of mutant and WT *Eh*-TPL was determined using 1–10 mmol·L^{-1} sodium pyruvate under optimal reaction conditions. Kinetic parameters (K_m, V_{max}, $k_{cat,}$ and k_{cat}/K_m) were calculated using the Lineweaver–Burk method (Table 2). The V_{max} value of mutant *Eh*-TPL was 42.6, 19.3% higher than that of WT *Eh*-TPL. The K_m value was reduced by 39.2% and the k_{cat}/K_m was enhanced twofold in the mutant. Sequence analysis revealed two mutated amino acids (S20C and N161S) in the 3-2F9 mutant enzyme. The three-dimensional structures of mutant and WT *Eh*-TPL were predicted using SWISS-MODEL (https://www.swissmodel.expasy.org/). In the *Eh*-TPL mutant, replacement of Ser-20 with a Cys residue in the N-terminal arm decreases the length of the hydrogen bond between Glu-23 and Arg-24 relative to that in the WT enzyme. In addition, two new hydrogen bonds are formed between Asp-159 and Ala-164 with Ser-161 in mutant *Eh*-TPL (Fig. 3). These additional interactions caused by amino acids' substitution (S20C and N161S) could explain the observed performance of mutant *Eh*-TPL, as shown in Fig. 2, in which the pH and temperature stability of mutant *Eh*-TPL were better than that of WT *Eh*-TPL.

Compared with WT *Eh*-TPL, the K_m value of mutant *Eh*-TPL was reduced and V_{max} was enhanced. This implied that the affinity of the mutant for the substrate was increased, which could accelerate the enzymatic reaction rate. Furthermore, based on the predicted three-dimensional structure, the enhanced catalytic performance and thermal and pH stability of the TPL mutant could be due to these two additional hydrogen bonds. The roles of amino acids in the β-elimination reaction catalyzed by TPL have been studied using site-directed mutagenesis based on the three-dimensional structure of TPL from *C. freundii* [4, 11]. However, the mechanism of the reversible L-DOPA synthesis reaction from catechol, sodium pyruvate, and ammonium acetate has

Table 3 Comparison of various strains for L-DOPA production with biocatalytic and fermentation routes in recent decades

Strain (enzyme)	Material (g L^{-1})	Process (bioreactor)	L-DOP (g L^{-1})	*Y* (100%)	*P* (g L^{-1} h^{-1})	Refs.
E. coli BL21 (*Eh*-TPL)	Catechol, ammonia, pyruvate	Bioconversion (5 L reactor)	69.10	85.74	11.52	This study
E. coli BL21 (PHAH)	Glucose	Fermentation (5 L fermenter)	25.53	–	0.53	[17]
E. coli DOPA-30 N (PHAH)	Glucose	Fermentation (5 L fermenter)	8.67	–	0.14	[50]
E. coli VH33tyrR (PHAH)	Glucose	Fermentation (1 L fermenter)	1.51	3.02	0.030	[18]
E. coli (Tyrosinase)	Glucose	Fermentation (3 L fermenter)	0.29	–	–	[31]
E. coli W3110 (PHAH)	Glycerol	Fermentation (5 L fermenter)	12.50	–	0.31	[10]
E. coli ATCC11105 (PHAH)	L-tyrosine	Bioconversion (shaking flask)	9.47	64.00	0.19	[24]
Acremonium rutilum (Tyrosinase)	L-tyrosine	Fermentation (shaking flask)	0.89	17.80	0.0093	[23]
Aspergillus oryzae ME_2 (Tyrosinase)	L-tyrosine	Bioconversion (shaking flask)	1.69	61.97	2.02	[1]
Yarrowia lipolytica (Tyrosinase)	L-tyrosine	Bioconversion (1.25 L reactor)	3.48	91.36	13.92	[2]
Bacillus sp. JPJ (Tyrosinase)	L-tyrosine	Bioconversion (shaking flask)	0.497	91.33	0.497	[43]
Brevundimonas sp. SGJ (Tyrosinase)	L-tyrosine	Bioconversion (shaking flask)	3.81	87.52	–	[44]
Erwinia herbicola (TPL)	Catechol, ammonia, pyruvate	Bioconversion (shaking flask)	15.00	83.74	15.00	[21]
Erwinia herbicola ATCC21434 (TPL)	Catechol, ammonia, pyruvate	Bioconversion (shaking flask)	58.50	–	1.22	[14]
E. coli (*Eh*-TPL)	Catechol, ammonia, pyruvate	Bioconversion (shaking flask)	20.70	45.65	0.69	[16]
E. coli (*Ss*-TPL)	Catechol, ammonia, pyruvate	Bioconversion (reactor)	29.80	–	4.97	[25]
E. coli (*Fn*-TPL)	Catechol, ammonia, pyruvate	Bioconversion (shaking flask)	110.00	87.70	5.24	[54]
E. coli (*Fn*-TPL)	Catechol, ammonia, pyruvate	Bioconversion (15 L reactor)	121.50	90.46	~4.67	[45]
Pseudomonas aeruginosa (*Cf*-TPL)	Catechol, ammonia, pyruvate	Bioconversion (shaking flask)	2.76	28.00	0.31	[33]

PHAH means *p*-hydroxyphenylacetate 3-hydroxylase; *Y* (100%), respectively, presents as quality conversion rate in fermentation processes (responding to substrate such as glucose, glycerol, or L-tyrosine) and molar conversion rate in bioconversion processes (responding to substrate such as L-tyrosine or catechol); *Eh*-/*Ss*-/*Fn*-/*Cf*-TPL means that the TPL originated from *Erwinia herbicola*, *Symbiobacterium* sp., *Fusobacterium nucleatum,* and *Citrobacter freundii*, respectively

not been reported, and this could be important for further increasing the titre of L-DOPA.

Application of mutant *Eh*-TPL for L-DOPA biosynthesis

High-density culturing of recombinant *E. coli* cells expressing the *Eh*-TPL mutant was performed using fed-batch mode in a 5 L fermenter. Biomass was collected by centrifuging and used for L-DOPA biosynthesis from sodium pyruvate, catechol, and ammonium acetate. A fed-batch mode was applied to control the catechol concentration; the flow rate of catechol and sodium pyruvate was 10 g L^{-1} h^{-1} and 12 g L^{-1} h^{-1}, respectively between 0 and 2 h; the flow rate of sodium pyruvate was unchanged, but the flow rate of catechol was changed to 7 g L^{-1} h^{-1} from 2 to 4 h, then adjusted to 4 g L^{-1} h^{-1} from 4 to 5 h. The results are shown in Fig. 4. The titre of L-DOPA reached 69.1 g L^{-1} after 6 h, the productivity was 11.52 g L^{-1}·h^{-1}, and the molar conversion rate from the catechol substrate

was 85.74%. Comparison of various strains for L-DOPA production in recent decades is presented in Table 3.

TPL from *E. herbicola* has extremely high activity and high L-DOPA productivity [21, 22]. The titre of L-DOPA using recombinant *E. coli* expressing *Eh*-TPL was low due to the toxicity of catechol [16, 30]. Catechol can denature proteins, irreversibly reducing the activity and stability of TPL [41]. The fed-batch mode can prevent substrate inhibition and enhance the titre of target products, and it has been widely employed in industrial production [42, 52]. The fed-batch mode established in this work solved the problem due to catechol toxicity, and high accumulation of L-DOPA was achieved. This approach provides a reference for optimising fermentation and/or whole-cell catalysis with substances that are toxic, harmful, or susceptible to causing inhibition.

Conclusions

In this study, a mutant *Eh*-TPL was generated by integrating error-prone PCR and high-throughput screening. The catalytic performance of the mutant was increased over a wider temperature and pH range, and the titre of L-DOPA was enhanced by 36.5% using whole-cell catalysis with recombinant *E. coli* BL21 (DE3) expressing mutant *Eh*-TPL in shake flasks. Finally, a fed-batch mode was established for whole-cell catalysis in a 5 L bioreactor, and the titre of L-DOPA reached 69.1 g L^{-1} with high productivity of 11.52 g L^{-1} h^{-1}. These results indicated that *Eh*-TPL mutant hold great potential for industrial L-DOPA production.

Acknowledgements This work was supported by the National Key Research and Development Program of China (2017YFC1600403), the National Natural Science Foundation of China (31830068, 21822806), the Fundamental Research Funds for the Central Universities (JUSRP51701A), the National First-class Discipline Program of Light Industry Technology and Engineering (LITE2018-08), and the Distinguished Professor Project of Jiangsu Province.

References

1. Ali S, Ikramul H (2006) Kinetic basis of celite (CM 2: 1) addition on the biosynthesis of 3,4-dihydroxyphenyl-L-alanine (L-DOPA) by *Aspergillus oryzae* ME2 using L-tyrosine as a basal substrate. World J Microb Biot 22:347–353. https://doi.org/10.1007/s11274-005-9040-1
2. Ali S, Shultz JL, Ikramul H (2007) High performance microbiological transformation of L-tyrosine to L-dopa by *Yarrowia lipolytica* NRRL-143. BMC Biotechnol 7:50. https://doi.org/10.1186/1472-6750-7-50
3. Balci H, Ozturk MT, Pijning T, Ozturk SI, Gumusel F (2014) Improved activity and pH stability of *E. coli* ATCC 11105 penicillin acylase by error-prone PCR. Appl Microbiol Biotechnol 98:4467–4477. https://doi.org/10.1007/s00253-013-5476-7
4. Barbolina MV, Kulikova VV, Tsvetikova MA, Anufrieva NV, Revtovich SV, Phillips RS, Gollnick PD, Demidkina TV, Faleev NG (2018) Serine 51 residue of *Citrobacter freundii* tyrosine phenol-lyase assists in C-alpha-proton abstraction and transfer in the reaction with substrate. Biochimie 147:63–69. https://doi.org/10.1016/j.biochi.2017.11.016
5. Ben Mabrouk S, Ayadi DZ, Ben Hlima H, Bejar S (2013) Thermostability improvement of maltogenic amylase MAUS149 by error prone PCR. J Biotechnol 168:601–606. https://doi.org/10.1016/j.jbiotec.2013.08.026
6. Calabrese VP (2007) Projected number of people with Parkinson disease in the most populous nations, 2005 through 2030. Neurology 69:223–224. https://doi.org/10.1212/01.wnl.0000271777.50910.73
7. Chandel M, Azmi W (2013) Purification and characterization of tyrosine phenol lyase from *Citrobacter freundii*. Appl Biochem Biotech 171:2040–2052. https://doi.org/10.1007/s12010-013-0491-9
8. Chaput JC, Woodbury NW, Stearns LA, Williams BAR (2008) Creating protein biocatalysts as tools for future industrial applications. Expert Opin Biol Th 8:1087–1098. https://doi.org/10.1517/14712590802181926
9. d'Oelsnitz S, Ellington A (2018) Continuous directed evolution for strain and protein engineering. Curr Opin Biotechnol 53:158–163. https://doi.org/10.1016/j.copbio.2017.12.029
10. Das A, Tyagi N, Verma A, Akhtar S, Mukherjee KJ (2018) Metabolic engineering of *Escherichia coli* W3110 strain by incorporating genome-level modifications and synthetic plasmid modules to enhance L-Dopa production from glycerol. Prep Biochem Biotech 48:671–682. https://doi.org/10.1080/10826068.2018.1487851
11. Demidkina TV, Antson AA, Faleev NG, Phillips RS, Zakomirdina LN (2009) Spatial structure and the mechanism of tyrosine phenol-lyase and tryptophan indole-lyase. Mol Biol 43:269–283. https://doi.org/10.1134/s0026893309020101
12. Denard CA, Ren H, Zhao H (2015) Improving and repurposing biocatalysts via directed evolution. Curr Opin Chem Biol 25:55–64. https://doi.org/10.1016/j.cbpa.2014.12.036
13. Dennig A, Busto E, Kroutil W, Faber K (2015) Biocatalytic one-pot synthesis of L-tyrosine derivatives from monosubstituted benzenes, pyruvate, and ammonia. ACS Catal 5:7503–7506. https://doi.org/10.1021/acscatal.5b02129
14. Enei H, Nakazawa H, Okumura S, Yamada H (1973) Synthesis of L-tyrosine or 3,4-dihydroxyphenyl-L-alanine from pyruvic acid, ammonia and phenol or pyrocatechol. Agr Bioi Chem 37:725–735
15. Etemadi F, Hashemi M, Randhir R, ZandVakili O, Ebadi A (2018) Accumulation of L-DOPA in various organs of faba bean and influence of drought, nitrogen stress, and processing methods on L-DOPA yield. Crop J 6:426–434. https://doi.org/10.1016/j.cj.2017.12.001
16. Foor F, Morin N, Bostian KA (1993) Production of L-dihydroxyphenylalanine in *Escherichia coli* with the tyrosine phenol-lyase gene cloned from *Erwinia*. Appl Environ Microbiol 59:3070–3075
17. Fordjour E, Adipah FK, Zhou S, Du G, Zhou J (2019) Metabolic engineering of *Escherichia coli* BL21 (DE3) for de novo production of L-DOPA from D-glucose. Microb Cell Fact 18:74. https://doi.org/10.1186/s12934-019-1122-0
18. Joyce Munoz A, Hernandez-Chavez G, de Anda R, Martinez A, Bolivar F, Gosset G (2011) Metabolic engineering of *Escherichia coli* for improving L-3,4-dihydroxyphenylalanine (L-DOPA) synthesis from glucose. J Ind Microbiol Biotechnol 38:1845–1852. https://doi.org/10.1007/s10295-011-0973-0
19. Katayama T, Suzuki H, Koyanagi T, Kumagai H (2000) Cloning and random mutagenesis of the *Erwinia herbicola* tyrR gene for high-level expression of tyrosine phenol-lyase. Appl Environ Microbiol 66:4764–4771. https://doi.org/10.1128/aem.66.11.4764-4771.2000

20. Kim S, Sung BH, Kim SC, Lee HS (2018) Genetic incorporation of L-dihydroxyphenylalanine (DOPA) biosynthesized by a tyrosine phenol-lyase. Chem Commun 54:3002–3005. https://doi.org/10.1039/c8cc00281a
21. Koyanagi T, Katayama T, Suzuki H, Nakazawa H, Yokozeki K, Kumagai H (2005) Effective production of 3,4-dihydroxyphenyl-L-alanine (L-DOPA) with *Erwinia herbicola* cells carrying a mutant transcriptional regulator TyrR. J Biotechnol 115:303–306. https://doi.org/10.1016/j.jbiotec.2004.08.016
22. Koyanagi T, Katayama T, Suzuki H, Onishi A, Yokozeki K, Kumagai H (2009) Hyperproduction of 3,4-Dihydroxyphenyl-L-alanine (L-Dopa) using *Erwinia herbicola* cells carrying a mutant transcriptional regulator TyrR. Biosci Biotech Bioch 73:1221–1223. https://doi.org/10.1271/bbb.90019
23. Krishnaveni R, Rathod V, Thakur MS, Neelgund YF (2009) Transformation of L-tyrosine to L-Dopa by a novel fungus, *Acremonium rutilum*, under submerged fermentation. Curr Microbiol 58:122–128. https://doi.org/10.1007/s00284-008-9287-5
24. Lee JY, Xun LY (1998) Novel biological process for L-DOPA production from L-tyrosine by *p*-hydroxyphenylacetate 3-hydroxylase. Biotechnol Lett 20:479–482. https://doi.org/10.1023/a:1005440229420
25. Lee SG, Ro HS, Hong SP, Kim EH, Sung MH (1996) Production of L-DOPA by thermostable tyrosine phenol-lyase of a thermophilic *Symbiobacterium* species overexpressed in recombinant *Escherichia coli*. J Microbiol Biotechn 6:98–102
26. Loiodice S, Young HW, Rion B, Meot B, Montagne P, Denibaud A-S, Viel R, La Rochelle CD (2019) Implication of nigral dopaminergic lesion and repeated L-dopa exposure in neuropsychiatric symptoms of Parkinson's disease. Behav Brain Res 360:120–127. https://doi.org/10.1016/j.bbr.2018.12.007
27. Longwell CK, Labanieh L, Cochran JR (2017) High-throughput screening technologies for enzyme engineering. Curr Opin Biotechnol 48:196–202. https://doi.org/10.1016/j.copbio.2017.05.012
28. Mayr LM, Bojanic D (2009) Novel trends in high-throughput screening. Curr Opin Pharmacol 9:580–588. https://doi.org/10.1016/j.coph.2009.08.004
29. Flickinge Michael C, Drew SW (1999) Fermentation, biocatalysis, and bioseparation. Encycl Bioprocess Technol 1:1–638
30. Min K, Park K, Park D-H, Yoo YJ (2015) Overview on the biotechnological production of L-DOPA. Appl Microbiol Biotechnol 99:575–584. https://doi.org/10.1007/s00253-014-6215-4
31. Nakagawa A, Minami H, Kim J-S, Koyanagi T, Katayama T, Sato F, Kumagai H (2011) A bacterial platform for fermentative production of plant alkaloids. Nat Commun 2:326. https://doi.org/10.1038/ncomms1327
32. Packer MS, Liu DR (2015) Methods for the directed evolution of proteins. Nat Rev Genet 16:379–394. https://doi.org/10.1038/nrg3927
33. Park HS, Lee JY, Kim HS (1998) Production of L-DOPA (3,4-dihydroxyphenyl-L-alanine) from benzene by using a hybrid pathway. Biotechnol Bioeng 58:339–343. https://doi.org/10.1002/(sici)1097-0290(19980420)58:2/3%3c339:aid-bit36%3e3.0.co;2-4
34. Phillips RS, Vita A, Spivey JB, Rudloff AP, Driscoll MD, Hay S (2016) Ground-state destabilization by Phe-448 and Phe-449 contributes to tyrosine phenol-lyase catalysis. ACS Catal 6:6770–6779. https://doi.org/10.1021/acscatal.6b01495
35. Randhir R, Shetty K (2004) Microwave-induced stimulation of L-DOPA, phenolics and antioxidant activity in fava bean (*Vicia faba*) for Parkinson's *diet*. Process Biochem 39:1775–1784. https://doi.org/10.1016/j.procbio.2003.08.006
36. Rolff M, Schottenheim J, Decker H, Tuczek F (2011) Copper-O-2 reactivity of tyrosinase models towards external monophenolic substrates: molecular mechanism and comparison with the enzyme. Chem Soc Rev 40:4077–4098. https://doi.org/10.1039/c0cs00202j
37. Savitskaya J, Protzko RJ, Li F-Z, Arkin AP, Dueber JE (2019) Iterative screening methodology enables isolation of strains with improved properties for a FACS-based screen and increased L-DOPA production. Sci Rep-UK 9:5815. https://doi.org/10.1038/s41598-019-41759-0
38. Sayyed IA, Sudalai A (2004) Asymmetric synthesis of L-DOPA and (R)-selegiline via, OsO_4-catalyzed asymmetric dihydroxylation. Tetrahedron-Asymmetr 15:3111–3116. https://doi.org/10.1016/j.tetasy.2004.08.007
39. Seisser B, Zinkl R, Gruber K, Kaufmann F, Hafner A, Kroutil W (2010) Cutting long syntheses short: access to non-natural tyrosine derivatives employing an engineered tyrosine phenol lyase. Adv Synth Catal 352:731–736. https://doi.org/10.1002/adsc.200900826
40. Seo J, Shin J-Y, Leijten J, Jeon O, Camci-Unal G, Dikina AD, Brinegar K, Ghaemmaghami AM, Alsberg E, Khademhosseini A (2018) High-throughput approaches for screening and analysis of cell behaviors. Biomaterials 153:85–101. https://doi.org/10.1016/j.biomaterials.2017.06.022
41. Stratford MRL, Ramsden CA, Riley PA (2013) Mechanistic studies of the inactivation of tyrosinase by resorcinol. Bioorgan Med Chem 21:1166–1173. https://doi.org/10.1016/j.bmc.2012.12.031
42. Sugiharto YEC, Harimawan A, Kresnowati MTAP, Purwadi R, Mariyana R, Andry Fitriana HN, Hosen HF (2016) Enzyme feeding strategies for better fed-batch enzymatic hydrolysis of empty fruit bunch. Bioresour Technol 207:175–179. https://doi.org/10.1016/j.biortech.2016.01.113
43. Surwase SN, Jadhav JP (2011) Bioconversion of L-tyrosine to L-DOPA by a novel bacterium *Bacillus* sp. JPJ. Amino Acids 41:495–506. https://doi.org/10.1007/s00726-010-0768-z
44. Surwase SN, Patil SA, Apine OA, Jadhav JP (2012) Efficient microbial conversion of L-tyrosine to L-DOPA by *Brevundimonas* sp. SGJ. Appl Biochem Biotech 167:1015–1028. https://doi.org/10.1007/s12010-012-9564-4
45. Tang X, Liu X, Suo H, Wang Z, Zheng R, Zheng Y (2018) Process development for efficient biosynthesis of L-DOPA with recombinant *Escherichia coli* harboring tyrosine phenol lyase from *Fusobacterium nucleatum*. Bioprocess Biosyst Eng 41:1347–1354. https://doi.org/10.1007/s00449-018-1962-8
46. Tang X, Suo H, Zheng R, Zheng Y (2018) An efficient colorimetric high-throughput screening method for synthetic activity of tyrosine phenol-lyase. Anal Biochem 560:7–11. https://doi.org/10.1016/j.ab.2018.08.026
47. Teshima N, Li JZ, Toda K, Dasgupta PK (2005) Determination of acetone in breath. Anal Chim Acta 535:189–199. https://doi.org/10.1016/j.aca.2004.12.018
48. Nagasaki Tomohisa, Sugita Masanori, Fukawa H (1973) Studies on DOPA transaminase of *Alcaligenes faecalis*. Agric Biol Chem 37:1701–1706
49. Valdes RH, Puzer L, Gomes M, Marques C, Aranda DAG, Bastos ML, Gemal AL, Antunes OAC (2004) Production of L-DOPA under heterogeneous asymmetric catalysis. Catal Commun 5:631–634. https://doi.org/10.1016/j.catcom.2004.07.018
50. Wei T, Cheng B, Liu J (2016) Genome engineering *Escherichia coli* for L-DOPA overproduction from glucose. Sci Rep-UK 6:30080. https://doi.org/10.1038/srep30080
51. Yamada H, Kumagai H (1975) Synthesis of L-tyrosine-related amino acids by beta-tyrosinase. Adv Appl Microbiol 19:249–288. https://doi.org/10.1016/s0065-2164(08)70431-3
52. Zeng W, Zhang H, Xu S, Fang F, Zhou J (2017) Biosynthesis of keto acids by fed-batch culture of *Yarrowia lipolytica* WSH-Z06.

Bioresour Technol 243:1037–1043. https://doi.org/10.1016/j.biortech.2017.07.063
53. Zhang Y, Zhou J, Du G, Chen J (2018) Purification and enzymatic properties of tyrosine phenol lyase from *Rhodobacter capsulatus*. Food Ferment Ind 44:13–19
54. Zheng R, Tang X, Suo H, Feng L, Liu X, Yang J, Zheng Y (2018) Biochemical characterization of a novel tyrosine phenol-lyase from *Fusobacterium nucleatum* for highly efficient biosynthesis of L-DOPA. Enzyme Microb Tech 112:88–93. https://doi.org/10.1016/j.enzmictec.2017.11.004